Cyclic performance of a precast beam-panel joint device

Prestazioni cicliche di un dispositivo di connessione trave-pannello

D. Sirtoli[1], P. Riva[2], A. Belleri[3], I. Becci[4]

[1,2,3] *Department of Civil Engineering, University of Bergamo, Bergamo, Italy*

[4] *allb s.r.l., Belforte del Chienti, Italy*

ABSTRACT: The recent earthquake of Amatrice in 2016 had a huge impact on both historical and recent buildings, underlining the needs of strengthening interventions against cyclic actions. Not just masonry buildings suffered the earthquake intensity but even precast industrial buildings showed local damages or even structural failure. For this type of constructions, a possible strengthening intervention is represented by the installation of anti-seismic connection devices. Depending on the connected elements and the device features, several improvements can be obtained. For instance, one of the issues in precast industrial buildings is represented by the cladding system, which is typically made by reinforced concrete panels with significant dimensions. In this paper, an experimental campaign on the cyclic response of a precast beam-panel joint device is proposed, evidencing its performance in cyclic tests and its capability in uncoupling the in-plane cladding system motion compared to the structural motion. / Il recente terremoto di Amatrice del 2016 ha avuto un forte impatto sulle costruzioni, sia storiche che di più recente concezione, sottolineando la necessità di interventi di rinforzo nei confronti di azioni cicliche. Non solo gli edifici in muratura hanno sofferto l'intensità del sisma, anche strutture prefabbricate quali capannoni industriali hanno mostrato danni locali fino a veri e propri collassi. Per quest'ultima tipologia strutturale, un possibile intervento di rinforzo è rappresentato dall'installazione di dispositivi di connessione antisismici. In funzione degli elementi strutturali connessi e delle caratteristiche stesse del dispositivo utilizzato, diversi sono i possibili miglioramenti ottenibili. Ad esempio, uno dei problemi riguardante gli edifici industriali prefabbricati sottoposti ad azioni cicliche è rappresentato dall'interazione tra struttura e pannelli di chiusura, i quali sono caratterizzati da una massa significativa. In questo articolo viene proposta una campagna sperimentale sulla risposta ciclica di un dispositivo di connessione trave-pannello, sottolineando le sue prestazioni per sollecitazioni cicliche e la sua capacità di disaccoppiare il moto nel piano dei pannelli perimetrali dal moto della struttura.

KEYWORDS: precast buildings; cladding panel connections; anti-seismic device; experimental campaign / edifici prefabbricati; connessione pannelli prefabbricati; dispositivi anti-sismici; campagna sperimentale.

INTRODUCTION

The Italian experience of the last decade on earthquake events underlined the need of strengthening interventions on structures against horizontal loads. Several constructive types were involved, from historical one-storey masonry buildings to multi-story RC ones. The main problem was the absence of specific connections/details against horizontal actions as those buildings were mainly designed just for gravity loads. Another constructive typology which was prticulary affected during the last earthquakes, especially Emilia 2012 and Amatrice 2016, were precast industrial and commercial buildings (Toniolo & Colombo 2012; Marzo et al. 2012; Savoia et al. 2012; Liberatore et al. 2013; Magliulo et al. 2014; Belleri et al. 2014; Bournas et al. 2014; Casotto et al. 2015; Minghini et al. 2016; Nastri et al. 2017; Palanci et al. 2017). Also these buildings were designed mainly against vertical loads, with connections between the elements, both structural and non-structural, not designed to carry seismic actions, and often relying solely on friction. It was observed that, during the seismic event, such connections are subjected to high loads and displacement demand, leading to their premature failure. The uncontrolled movement of each part of the structure produces a detrimental effect on the overall building, often leading to partial collapses. In this case, one of the possible solutions is represented by the provision of additional restraints. Depending on the design purposes, several types of devices can be used, like rigid connection devices, displacement dependent devices, velocity dependent devices, isolators or a combination of them, and more.

In this paper, a new device to connect vertical cladding panels and supporting beams, certified as a guide bearing/mobile permanent connection device

(EN 1337-8:2007), is considered, evidencing its experimental performance in cyclic tests and its capability of uncoupling the in-plane cladding system and the structural motions. In such a way the panel behaves like a pendulum according with the safe-cladding project terminology (Toniolo & Dal Lago 2017). This last effect is of importance in precast buildings because of the dimensions of these elements, which are related to the mass involved in the motion during the seismic event (Colombo et al. 2014, Fischinger et al. 2014, Zoubek et al. 2016, Pantoli et al. 2016, Belleri et al. 2016, Belleri et al. 2017). The possibility to uncouple the concrete panels and the main frame can lead to a strong decrease of the seismic force transferred to the main structure (Dal Lago & Lamperti Tornaghi 2018), with a direct benefit on the building damage. In terms of cyclic tests, both out-plane and in-plane directions were investigated. In the first one the friction mechanism of the device is studied in two different configurations, while, in the second one, the sliding feature of the device is evidenced, changing the preload applied to the system, showing its effect on the force required to allow sliding.

DEVICE DESCRIPTION

Components identification

The studied device is composed of six macro-elements, as shown in Figure 1, identified with letters, from "A" to "F", as follow:

- A) Panel connection element;
- B) Beam connection element;
- C) Joint rocker;
- D) Rocker guide-rod;
- E) Sliding collar;
- F) Rocker clamping jaws.

Figure 2 proposes an exploded view of the joint rocker details and its sliding mechanism.

The device resistant mechanism is composed of the following elements: "A" and "B" act as restraints to the panel and the beam, respectively. These independent elements are connected together by the rocker "C". On the beam side, two threaded bars connect "B" to "C", from the rod "C5" on the rocker to the collars on the beam connection element "B". On the panel side the guide rod "D", restrained by the elements "A" to the panel, presents a sliding collar ("E") provided with two screws at its edge. These are the elements that connect the panel system to "C1".

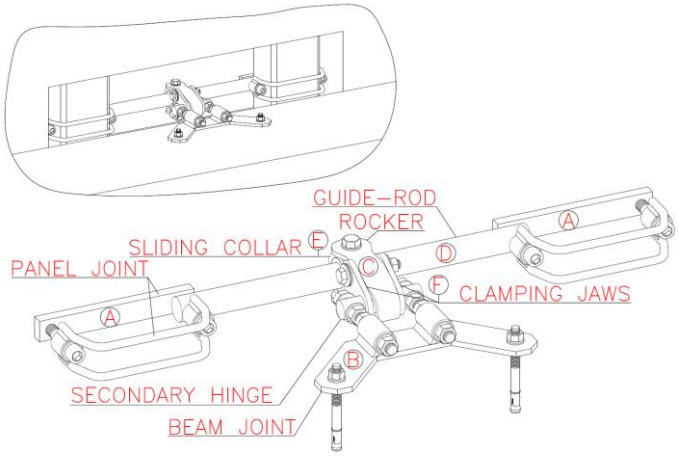

Figure 1. Main elements making up the connection / Principali elementi costituenti la connessione

Considering the sliding mechanism between "C" and "F", this is governed by the clamping force generated by two bolts. As the elements "F7"-"C5" are designed to have a gap in the inner part of "C1", the force at which "F" is clamped to "C" is of crucial importance as it governs the device sliding mechanism. In order to keep constant the clamping jaws tightening torque during the sliding movement, 3 cup springs are placed at each bolt side.

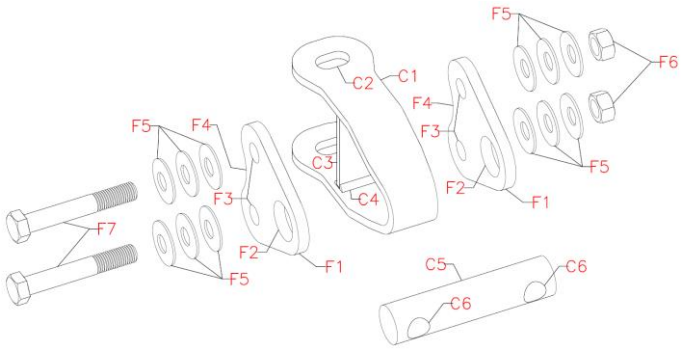

Figure 2. Exploded view of the joint rocker and its clamping jaws / Esploso dell'elemento carrello

Kinematics

The device accepts little distortions from its undeformed configuration without affecting the resistant mechanism. These configurations can be reconnected to tolerance issues, beam deflection, rocking effect, beam/panel displacement and so on.

The main joint kinematic allowed is as follows:

1_Relative displacement kinematism between beam and panel in the vertical plane (Figure 3a)

2_Angular distortion kinematism in the vertical plane, parallel to the main panel plane (Figure 3b);

3_Relative displacement kinematism between beam and panel in the horizontal plane (Figure 3c);

Considering the vertical plane kinematism, the angular distortion "VDA" is produced from a beam deflection or the panels rocking effect with respect to the main structures or an assembly defect with a

not perfectly horizontal guide-rod. The maximum acceptable value for this defect is 3 cm, considered as the algebraic sum of the different contributions. In terms of relative vertical displacement between beam and panel, it can be produced from a beam deflection due to a seismic action or a vertical settlement of the panel supports. This deviation is calculated on the vertical distance between the two device centers of rotation; the designed tolerance is ±5 cm. In order to reach this value, a horizontal distance between beam and panel in the undeformed configuration of 1.2 cm has to be considered.

Concerning the kinematism in the horizontal plane, usually it is caused by the different seismic response of the structural elements. In the parallel direction to the main panel plane, the device allows relative displacements, decoupling beam and panel movements. Differently, in the perpendicular direction to the main panel plane, the displacement is blocked and the seismic action is transferred by the device strength capacity.

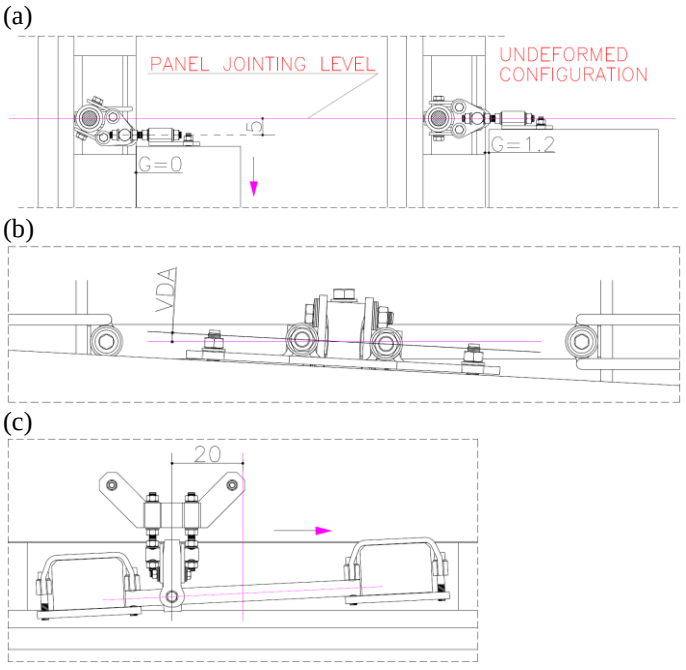

Figure 3. Device kinematics: (a) relative displacement, (b) angular distorsion and (c) mounting defect / Cinematismi del dispositivo: (a) spostamento relativo, (b) distorsione angolare e (c) difetto di montaggio.

SET-UP CONFIGURATION

Test parameters definition

Based on the device kinematics previously described, three different configurations were defined for the test set-up; two were aimed at the device characterization (Figure 4a-b) and one to its investigation in a real scale test (Figure 4c). In the first configuration (Figure 4a) the sliding mechanism between clamping jaws and joint rocker was investigated, setting the test in displacement control mode for a range equal to the tolerance between “F7”-“C5” and “C1” (12.8 mm) at a speed of 12 mm/min. In order to evaluate the device hysteretic behavior, 10 cycles were considered in the test parameter definition.

In the second set-up configuration (Figure 4b) the entire device was analyzed, testing its resistant capacity to a horizontal plane load applied perpendicularly to the guide-rod axis. Even in this configuration the number of cycles was set to 10 in order to evaluate its hysteretic behavior. The test was carried out in force control. This difference was required in order to have independent results from the activation of the sliding mechanism. The design resistance force was set to 50 kN, reached cyclically ten times in both load directions, at a speed of 2 kN/sec.

Eventually, a test on a real scale element was defined (Figure 4c) in order to evaluate the device capacity to slide until the design displacement when subjected to the design force, defined with the second set-up configuration. The test simulates the real application conditions at which the device will be subjected.

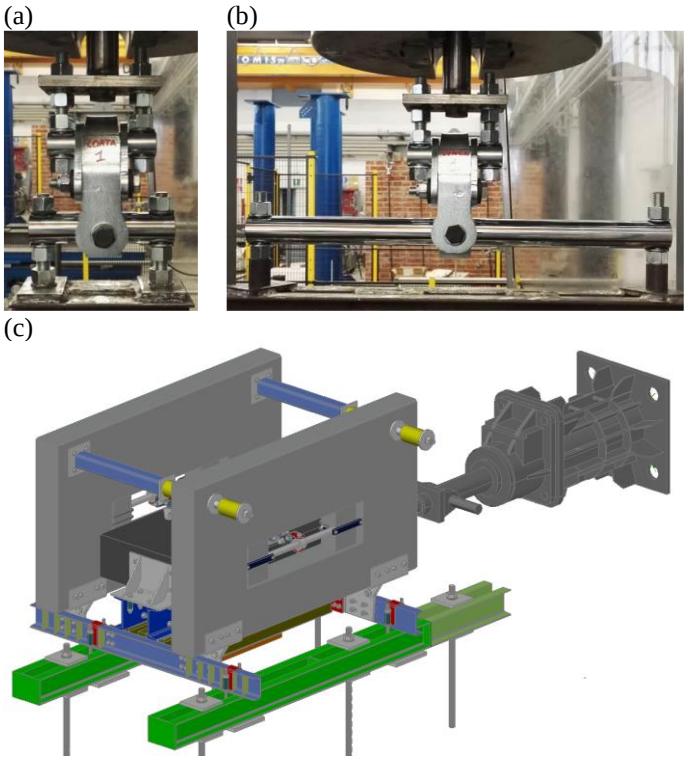

Figure 4. Test set-up for the device characterization (a, b) and real scale test (c) / Configurazioni del banco prova per la caratterizzazione del dispositivo (a, b) e prova in scala reale (c).

Figure 4c shows the set-up designed to test the device. A steel beams system, anchored to the floor by pre-tensioned steel bars, supports three concrete elements, two representing the panels and one for the beam. While the panels are sustained by four hinges, two for each panel, allowing rotation movement, the beam is placed on a rocker, able to move in one di-

rection (along the longitudinal panel plane, corresponding to the longitudinal guide-rod axis). This latter element is bonded to the electromechanical jack which applies the displacement during the test. Beam and panels are connected to each other just by the device. In order to simulate the panel weight during seismic actions, a horizontal constant preload is applied to the device by hydraulic jacks placed at the top of the panels. Three different preload levels were considered: the unloaded condition, 30 kN and 50 kN, the latter representing the design force value. Five cycles were considered during the test; the first at ±5 cm, the second at ±10 cm and then a triplet at the design displacement of ±20 cm. The test was done in displacement control at a speed of 0.7 mm/sec.

Instrumentation

The first two tests were carried out using a hydraulic Universal testing machine. The load and the displacement were recorded directly by the load cell and displacement transducer of the machine. For these two tests, no additional instruments were considered.

For the real scale test several instruments were used. The relative displacement between beam and panels was applied with an electromechanical jack, fixed to the laboratory reaction wall, of maximum capacity of 1000kN. Its stroke was monitored with a 100 cm wire potentiometric transducer (Figure 5a) placed at the end of the beam, on the same axis of the electromechanical jack, while the force required to slide the beam was recorded with a 100 kN load cell placed in between the jack and the set-up (Figure 5b). The preload was applied with four hydraulic jacks (a parallel couple composed each of two jacks in series) positioned at the two top sides of the panels at a height of 112 cm respect to the hinge at the base of the panels (Figure 5c). The hydraulic force was acquired with a pressure transducer placed on the pump unit. As the device is mounted at 60 cm height, the hydraulic system applied force was defined in order to generate the right preload for the single device. Similarly, the opening between the two panels was recorded by a 20 cm spring potentiometric transducer (Figure 5c) placed in the middle of the panels at a height, compared to the same hinge, of 122 cm.

(a)

(b)

(c)

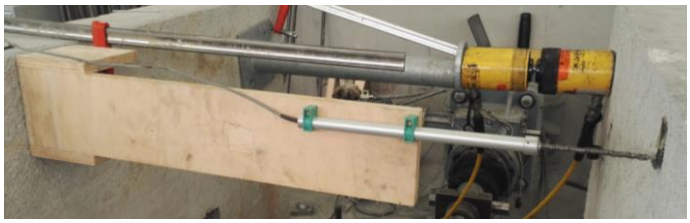

Figure 5. Real scale test instruments: wire potentiometric transducer (a), load cell (b), hydraulic jacks (c) and spring potentiometric transducer (c) / Strumenti della prova in scala reale: strumento a filo (a), cella di carico (b), martinetti idraulici (c) e tastatore a molla (c).

EXPERIMENTAL RESULTS

Short guide-rod device

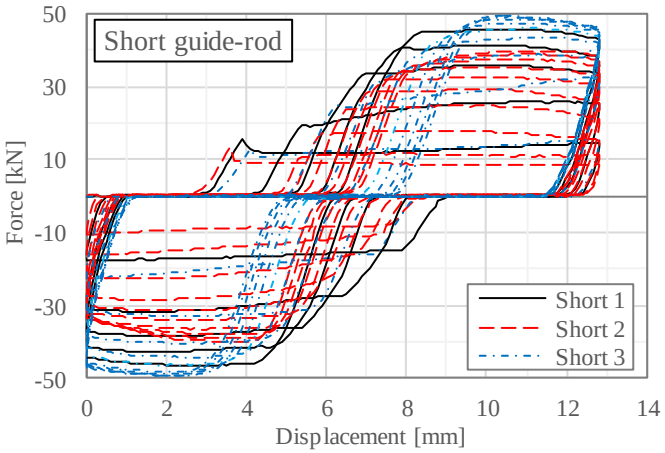

Figure 6. Comparison graph of the three tested samples in the short guide-rod set-up / Grafico di confronto del comportamento dei tre dispositivi nella configurazione a guida corta

The results of the three devices tested on the short guide-rod are shown in Figure 6.

A strong dependency between performance stability and number of cycles performed is observed. At the beginning of the test the two clamping jaws “F” start to slide already at low applied force levels. By the number of cycles, the activation of the resistant mechanism shifts at higher displacement values, showing either an increase of the correspondent sliding force. This trend tends to stabilize with the number of cycles performed.

The same behavior was obtained in the two samples tested for ten cycles, with the only difference in the higher stability reached during the final cycles.

From the comparison graph between the three samples, a good accordance can be seen between the collected results, with a maximum resistant force between 40 and 50 kN during the final cycle.

Long guide-rod device

The behavior of the three samples tested with the long guide-rod set-up, with the joint rocker “C” positioned in the middle of the guide, are shown in Figure 7.

Following the indications obtained in the short guide-rod tests, the number of cycles set was set equal to 10. It is worth noting that the results were obtained from force-controlled tests.

The initial device configuration was chosen in order to have an unloaded system without any tolerance between bolts "F7" and element "C1" at the beginning of the test. In this way, graphs from different tests become easier to compare.

The shape of the curve at different cycles underlines the combination of two main aspects in the global behavior definition; the flexural strength of the guide-rod "D1" and the friction evolution of the rocker "C" (relative sliding between clamping jaws "F1" and element "C1"). Representative is the behavior of the second sample (Long 2, red dotted line) where the friction mechanism activated just on the first loading branch of the first cycle, remaining stable thereafter. This test evidenced the relation between force and displacement in the case in which the only resistant mechanism is represented by the flexural strength of the guide-rod. Results show the stability of this element during the cyclic test, with a slight increment of displacement and a small decrease of stiffness.

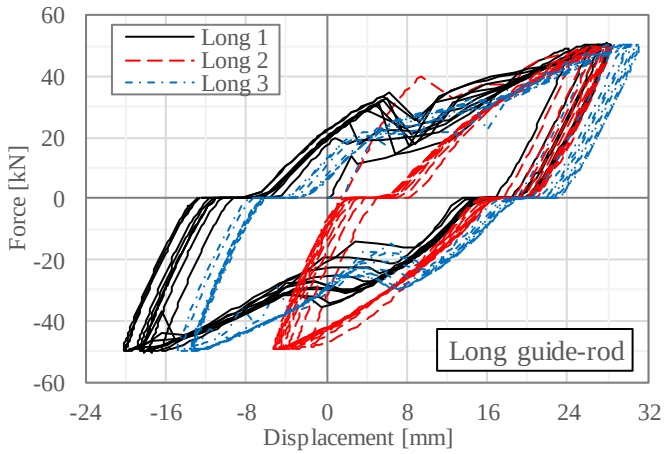

Figure 7. Comparison graph of the three tested samples in the long guide-rod set-up / Grafico di confronto del comportamento dei tre dispositivi nella configurazione a guida lunga

Considering the first and third samples behavior, they draw a similar shape of the force-displacement curve compared to the second sample, especially at the two edges. This stable behavior is representative of the guide-rod flexural strength, which contribute to the strength definition of the device. The difference between the three samples is mainly due to the activation or not of the friction mechanism. This phenomenon does not change consistently the evolution of the graph in terms of force but it modifies its extension in terms of displacement. The sliding effect is drawn on the graph as a translation of the curve where the friction is activated. This mechanism is of fundamental importance for the device capacity in energy dissipation and adaptive features; thanks to this sliding movement, a defect in the assembly operation can be accepted without interfere with the device properties.

The final comparison between the three long guide-rod samples (Figure 7) underlines what said above. All the curves are composed of two contributions: "D1" flexural strength and "C" friction mechanism. While the first is stable and gives a constant contribution to the device behavior, the second represents a variable effect, which can be activated or not.

Full scale test

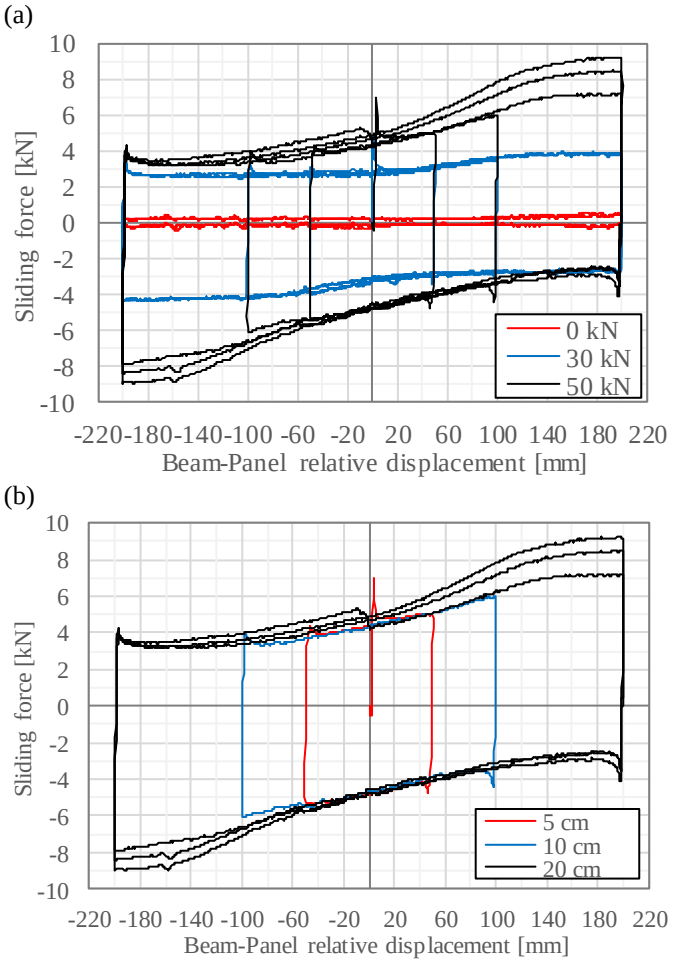

Figure 8. Results from the cyclic test on the full scale element in terms of applied preload (a) focusing on the 50kN test (b) / Risultati delle prove cicliche sull'elemento in scala reale in funzione del precarico applicato (a) evidenziando i risultati a 50 kN (b).

The sliding force required to move the system is plotted in Figure 8a-b. The first graph shows a comparison between the overall tests done at different preload of 0, 30 and 50 kN. While the second reports the five cycles done with the device preloaded at 50 kN, distinguishing between the three displacement levels of 5, 10 and 20 cm.

The initial set-up configuration is organized to have a distance between beam and panel of 1.2 cm; this gap represents the design value at which the device allows the vertical kinematism described in paragraph **Errore. L'origine riferimento non è stata**

trovata., consisting in the relative vertical displacement between beam and panel of ±5 cm. The two elements "A" are fixed to the little concrete pillars in order to create a perfectly horizontal line between the two device rotation centers (the guide-rod "D1" and the second hinge-rod "C5"). Eventually, the collar "E1" is positioned in the middle of the guide-rod and the whole system is preloaded before starting the cycles.

The preload was corrected manually just once, at the second 20 cm cycle. After the first application of load, the friction mechanism gets activated at above 40 kN load, reaching 1.8 cm stroke at the end of the first cycle at ±5 cm. The device displacement increases thereafter until 30 mm at the final test cycle, which is a similar value to the test on the long guide-rod performed with the universal testing machine, confirming the device behavior.

Considering the sliding force recorded during the test, the results show an increase as the collar go to higher displacement levels. During the first cycle at ±5 cm the required force to move the collar slightly varied from 4 to 5 kN, increasing from lower to higher displacement level. The same trend was evidenced at the second cycle at ±10 cm, where the sliding force varied from 3.5 to 6 kN following the same curve as in the previous cycle. The cycles at ±20 cm evidenced the first variation from the trend recorded so far, with a similar general behavior, but with an increment in the sliding force at the same displacement level compared to the previous cycles. Considering the positive direction, from the first to the third cycle at 20 cm the force changed from 7 to 9 kN while, in the negative direction, changed from 8 to 9 kN. Considering the only maximum force value reached in both directions at the design displacement level of 20 cm, it represents the 18% of the applied preload.

From the comparison proposed in Figure 8a of the sliding force evolution at the three considered preload levels, it is possible to evidence a correlation between these two parameters. An increase in the applied preload cause an increase of the force required to move the collar on the guide-rod. Moreover, an increase in the preload causes the curve shape to be similar to that at 50 kN, where the low displacement levels are related to a lower sliding force. Considering the unloaded configuration, small levels of sliding force are recorded, reaching less than 0.5 kN to move the device.

CONCLUSIONS

In this research, the cyclic performance of a guide bearing/mobile permanent connection device was studied. Three different configurations were considered: two small scale tests, investigating the out-of-plane performance in terms of friction mechanism (short guide rod) and flexural behavior of the metallic rod (long guide rod), and a final real scale test, evidencing the realistic in-plane behavior.

The friction mechanism designed showed an increasing results stability by increasing the number of cycles. The trend is to increase the friction force at each passage from the same point, with a decreasing gradient between two subsequent cycles. This mechanism is involved in the flexural behavior of the metallic rod. As the flexural response of this element can be considered stable between the three analyzed samples, what changes the behavior is the force at which the clamping jaws start to slide. This force, as said before, tends to increase by the number of cycles. These performances are useful especially for the device adaptive skills during erection, where assembly mistakes are common.

Considering the on-site behavior of the device, a nearly zero sliding force was recorded with the unloaded sample. This force tends to increase with the applied load, reaching a maximum at the edges of the rod. At a preload of 50 kN the sliding force reported a minimum of 4 kN and a maximum of 9 kN.

Thanks to the designed kinematics, this device can adapt to several different situations, maintaining its performance and its main aim of uncoupling the beam-panel motion.

In questa ricerca, le prestazioni cicliche di un dispositivo di collegamento guida/mobile permanente sono state studiate. Tre configurazioni differenti sono state considerate: due in scala ridotta per studiare le prestazioni fuori piano in termini di meccanismo attritivo (guida corta) e comportamento a flessione della guida metallica (guida lunga), e una prova finale in scala reale che evidenzi il comportamento nel piano, in condizioni realistiche, del dispositivo.

Il meccanismo ad attrito ha mostrato un aumento della stabilità dei risultati con l'aumentare del numero di cicli a cui è sottoposto. La tendenza è quella di un aumento della forza di attrito ad ogni passaggio per uno stesso punto, con un calo del gradiente tra due cicli successivi. Questo meccanismo è coinvolto anche nel comportamento a flessione della guida metallica. Dato che la risposta in flessione di questo elemento può essere considerata stabile tra i campioni testati, ciò che cambia il loro comportamento è la forza alla quale le piastre di serraggio iniziano a scorrere. Questa forza, come detto in precedenza, tende ad incrementare con il numero di cicli eseguiti, quindi, può mostrarsi inizialmente e stabilizzarsi in seguito, come riportato dal campione "Long 2". Queste prestazioni sono specialmente utili ai fini delle capacità adattive del dispositivo alle condizioni reali di cantiere, dove difetti di montaggio capitano spesso.

Considerando il comportamento del dispositivo nella configurazione di prova in scala reale, a campione scarico è stata registrata una forza di scorrimento quasi nulla. Questa tende ad aumentare con il precarico applicato, raggiungendo un massimo alle estremità della guida. A precarico di 50 kN è stata registrata una forza di scorrimento minima di 4 kN e massima di 9 kN. Grazie ai cinematismi progettati, il dispositivo riesce ad adattarsi ad una moltitudine di situazioni differenti, mantenendo le

sue prestazioni e il suo fine ultimo di disaccoppiare il movimento tra trave e pannello.

REFERENCES

Belleri, A. Brunesi, E. Nascimbene, R. Pagani, M. Riva, P. 2014. Seismic Performance of Precast Industrial Facilities Following Major Earthquakes in the Italian Territory. *J. Perform. Constr. Facil.,* doi:10.1061/(ASCE)CF.1943-5509.0000617

Belleri, A. Cornali, F. Passoni, C. Marini, A. Riva, P. 2017. Evaluation of out-of-plane seismic performance of column-to-column precast concrete cladding panels in one-storey industrial buildings. *Journal of Earthquake Engineering and Structural Dynamics*, 47: 397-417

Belleri, A. Torquati, M. Marini, A. Riva, P. 2016 Horizontal cladding panels: in-plane seismic performance in precast concrete buildings. *Bulletin of Earthquake Engineering*, doi:10.1007/s10518-015-9861-8

Bournas, D.A. Negro, P. Taucer, F.F. 2014. Performance of industrial buildings during the Emilia earthquakes in Northern Italy and recommendations for their strengthening. *Bulletin of Earthquake Engineering*, 12(5):2383-2404

Casotto, C. Silva, V. Crowley, H. Nascimbene, R. Pinho, R. 2015. Seismic Fragility of Italian RC Precast Industrial Structures. *Engineering Structures*, 94:122-136

Colombo. A, Negro. P, Toniolo. G, Lamperti. M. 2016. Design guidelines for precast structures with cladding panels, *JRC Technical report*, ISBN 978-92-79-58534-0

Dal Lago, B. Lamperti Tornaghi, M. 2018. Sliding channel cladding connections for precast structures subjected to earthquake action. *Bull Earthquake Eng*, 16, 5621–5646

Fischinger, M. Zoubek, B. Isakovic, T. 2014. Seismic response of precast industrial buildings. *Perspectives on European Earthquake Engineering and Seismology*: Vol. 1. Ansal A (editor), Springer, Berlin, pp 131-177

Liberatore, L. Sorrentino, L. Liberatore, D. Decanini, L.D. 2013. Failure of industrial structures induced by the Emilia (Italy) 2012 earthquakes. *Engineering Failure Analysis*, 34:629-647

Magliulo, G. Ercolino, M. Petrone, C. Coppola, O. Manfredi, G. 2014. The Emilia Earthquake: Seismic Performance of Precast Reinforced Concrete Buildings. *Earthquake Spectra*, 30(2):891-912

Marzo A, Marghella G, Indirli M (2012) The Emilia-Romagna earthquake: damages to precast/prestressed reinforced concrete factories. *Ingegneria Sismica*, 29(2):132-147

Minghini F, Ongaretto E, Ligabue V, Savoia M, Tullini N (2016) Observational failure analysis of precast buildings after the 2012 Emilia earthquakes. *Earthquake and Structures*, 11(2):327-346

Nastri E, Vergato M, Latour M (2017) Performance evaluation of a seismic retrofitted R.C. precast industrial building. *Earthquakes and Structures*, Vol. 12, No. 1 (2017) 13-21

Palanci M, Senel SM, Kalkan A (2017) Assessment of one story existing precast industrial buildings in Turkey based on fragility curves. *Bulletin of Earthquake Engineering*, 15(1):271-289

Pantoli E, Hutchinson TC, McMullin KM, Underwood GA, Hildebrand MJ (2016) Seismic-drift-compatible design of architectural precast concrete cladding: tieback connections and corner joints. *PCI journal*, 61(4):38-52

Savoia M, Mazzotti C, Buratti N, Ferracuti B, Bovo M, Ligabue V, Vincenzi L (2012) Damages and collapses in industrial precast buildings after the Emilia earthquake. *Ingegneria Sismica*, 29(2-3):120-131

Toniolo, G. Colombo, A. 2012. Precast concrete structures: the lessons learned from the L'Aquila earthquake. *Structural Concrete*, 13(2):73-83

Toniolo, G. Dal Lago, B. 2017. Conceptual design and full-scale experimentation of cladding panel connection systems of precast buildings. *Earthquake Engineering & Structural Dynamics*, 46(14): 2565-2586

Zoubek, B. Fischinger, M. Isaković, T. 2016. Cyclic response of hammer-head strap cladding-to-structure connections used in RC precast building, *Engineering Structures*, 119:135-148